symmetry

MDPI

Article

On the Effect of Thomson and Initial Stress in a Thermo-Porous Elastic Solid under G-N Electromagnetic Theory

Elsayed M. Abd-Elaziz [1], Marin Marin [2,*] and Mohamed I. A. Othman [3]

[1] Zagazig Higher Institute of Engineering & Technology, Ministry of Higher Education, P.O. Box 44519, Zagazig, Egypt; sayed_nr@yahoo.com
[2] Department of Mathematics and Computer Science, Transilvania University of Brasov, Brasov 500036, Romania
[3] Department of Mathematics, Faculty of Science, Zagazig University, P.O. Box 44519, Zagazig, Egypt; m_i_a_othman@yahoo.com
* Correspondence: m.marin@unitbv.ro

Received: 22 January 2019; Accepted: 14 March 2019; Published: 20 March 2019

Abstract: The present work investigated the effect of Thomson and initial stress in a thermo-porous elastic solid under G-N electromagnetic theory. The Thomson coefficient affects the heat condition equation. A constant Thomson coefficient, instead of traditionally a constant Seebeck coefficient, is assumed. The charge density of the induced electric current is taken as a function of time. A normal mode method is proposed to analyze the problem and to obtain numerical solutions. The results that were obtained for all physical sizes are graphically illustrated and we offer a comparison between the type II G-N theory and the G-N theory of type III, both in the present case and in the absence of specific parameters, as initial stress, pores and the Thomson effect. Some particular cases are also discussed in the context of the problem. The results indicate that the effect of initial stress, Thomson coefficient effect, and magnetic field are very pronounced.

Keywords: Thomson effect; initial stress; magneto-thermoelastic; voids; normal mode method; G-N theory

1. Introduction

In the generalized theories, the governing equations involve thermal relaxation times and they are of the hyperbolic type. Green and Naghdi [1–3] considered a new extend theory by including the thermal displacement gradient between the constitutive variables. As we know, the classically coupled thermoelasticity includes the temperature gradient as one of the constitutive variables.

An important feature of this theory is that it does not accommodate the dissipation of thermal energy. In paper by Sharma and Chauhan [4], we find an approach regarding the elastic interactions without considering the energy dissipation due to heat sources and body forces.

An important step in evolution of the classical theory of elasticity was made through the appearance of the theory of poroelasticity, which consider the volume of void, in an elastic body with pores, as a kinematics variable.

This gave the opportunity to investigate some concrete types of biological and geological solids and their useful applications. See, for instance, the applications in the fuel-cell industry [5–10].

We have to point out that the theory of linear elastic bodies with pores allows for the approach of such properties of biological and geological medium that could not be studied in the context of classical theory. It is very important to note that, when the volume of the pores tends to zero, we can see that the poroelastic theory reduces to the theory of classical elasticity.

In the paper, Nunziato and Cowin [11] first established a theory of elastic bodies with pores in the non-linear theory case.

This theory of porous media has gained a great extension over the last period of time, and many authors consider different mathematical models for the mechanical behavior of solids with pores, by combining the poroelasticity theory with other different theories, in other words, combining different effects, [12–16].

The consideration of the dynamic reaction of a thermoelastic body with additional parameters is very helpful in solving many concrete applications. For instance, the initial stresses are considered in a thermoelastic body with pores due to different reasons, such as the gravity variations, the difference of temperature, the process of quenching, etc.

Clearly, the earth is constantly under the influence of high initial stresses. As such, the researchers have allocated great importance to the study the effect of initial stresses regarding the thermal and mechanical state of a solid. For instance, Montanaro in [17] investigated a thermoelastic isotropic body with hydrostatic initial stress.

Of course, the laser pulse has an effect on thermal loading in an elastic body with voids. Othman and Abd-Elaziz studied this effect in the paper [18]. Marin investigated Cesaro means in the thermoelasticity of dipolar bodies [19]. Marin and Oechsner studied the effect of a dipolar structure on the Holder stability in Green-Naghdi thermoelasticity [20].

Other effects, such as the effect of the Earth's electromagnetic field on seismic propagations, the designing of different elements of machine, emissions of electromagnetic radiations from nuclear devices, plasma physics, etc., can be found in [21–27].

In our present study, we approach of the plane strain problem of a half-space body consisting of an electro-magneto-thermoelastic material that possesses voids and is subjected to some initial stress and to the Thomson effect. Our mathematical model is regarding the Green–Naghdi theory of type II and III of thermoelasticity. We assume that the Thomson effect is a constant coefficient and the density of charges that are induced by electric current is a function that depends on time variable.

In order to obtain the expressions for the considered parameters, it used the known normal mode technique. We also have obtained some graphic representations for the repartition of the considered variables.

2. Formulation of the Problem

An isotropic and homogeneous elastic body with pores (voids) is considered, with the temperature T_0, in the reference state, and the half space $(y \geq 0)$. The motion referred to a rectangular Cartesian system of coordinates (x, y, z) with origins in the surface $(z = 0)$. Additionally, the X-axis is pointing vertically into the body. In the of a two-dimensional problem, we suppose that the evolution of the body will be characterized by the displacement vector $\boldsymbol{u}$, with components $\boldsymbol{u} = (u, v, 0)$. The functions that are considered in this context are dependent on the time variable t and of the spatial variables x and y.

We consider a magnetic field with components $\boldsymbol{H} = (0, 0, H_3)$, having a constant intensity, which acts parallel to the direction of the Z-axis.

It is known that a magnetic field of the form $\boldsymbol{H} = (0, 0, H_0 + h(x, y, t))$ produces an induced electric field of components $\boldsymbol{E} = (E_1, E_2, 0)$, and an induced magnetic field, as denoted by $\boldsymbol{h}$, and these satisfy the electromagnetism equations, in the linearized form. We will use the Maxwell's equations [24] in order to characterize the evolution of the electric field and for variation of the magnetic field, as follows:

$$\nabla \times \boldsymbol{h} = \boldsymbol{J} + \dot{\boldsymbol{D}}, \tag{1}$$

$$\nabla \times \boldsymbol{E} = -\dot{\boldsymbol{B}}, \tag{2}$$

$$\nabla . \boldsymbol{B} = 0, \ \nabla . \boldsymbol{D} = \rho_e, \tag{3}$$

$$\boldsymbol{B} = \mu_0 (\boldsymbol{H} + \boldsymbol{h}), \ \boldsymbol{D} = \varepsilon_0 \boldsymbol{E}. \tag{4}$$

The modified Ohm's law for a medium with finite conductivity supplements the above system of coupled equations, namely

$$\boldsymbol{J} = \sigma_0(\boldsymbol{E} + \mu_0 \dot{\boldsymbol{u}} \times \boldsymbol{H}), \tag{5}$$

where μ_0 is the magnetic permeability, $\boldsymbol{B}$ is the magnetic displacement vector, ε_0 is the electric permeability, $\boldsymbol{J}$ is the current density vector, ρ_e is the charge density, $\boldsymbol{D}$ is the electric displacement vector, and $\boldsymbol{E}$ is the induced electric field vector.

For an isotropic and homogeneous thermoelastic body having pores, the constitutive equations receive the following form:

$$\sigma_{ij} = 2\mu\, e_{ij} + (\lambda\, e_{rr} + \lambda_0 \ \phi - \beta\, T\,)\delta_{ij} - L^*(\delta_{ij} + m^*_{ij}), \tag{6}$$

$$h_i = \alpha \phi_{,i}, \tag{7}$$

$$g = -\lambda_0\, e_{rr} - \xi_1\, \varphi + mT, \tag{8}$$

$$\rho\eta^* = \beta e_{rr} + a_0\, T + m\phi. \tag{9}$$

The strain-displacement relation is

$$e_{ij} = \frac{1}{2}(u_{i,j} + u_{j,i}). \tag{10}$$

The tensor of rotation has the components:

$$m^*_{ij} = \frac{1}{2}(u_{j,i} - u_{i,j}),\ i, j = 1, 2, 3. \tag{11}$$

In Green-Naghdi (G-N) theories we take into account the Thomson effect, so that the Fourier's law becomes

$$q_i = -\left[kT_{,i} + k^*\, \dot{T}_{,i}\right] + MJ_i, \tag{12}$$

which gives

$$q_{i,i} = -\left[kT_{,ii} + k^*\, \dot{T}_{,ii}\right] + M\, J_{i,i}. \tag{13}$$

If we take into account Equations (1) and (3), then from Equation (13), we deduce

$$q_{i,i} = -\left[kT_{,ii} + k^*\, \dot{T}_{,ii}\,\right] + M\, \dot{\rho}_e. \tag{14}$$

where T is the temperature above the reference temperature T_0 is chosen so that $|(T - T_0)/T_0| < 1$, λ, μ are the counterparts of Lame' constants, t is the time, σ_{ij} are the components of the stress tensor, $h_{,i}$ is the equilibrated stress vector, ψ is the equilibrated inertia, g is the intrinsic equilibrated body force, α, λ_0, ξ_1, ω_0, m are constants of material that are due to the presence of the pores, $\beta = (3\,\lambda + 2\,\mu)\,\alpha_t$, such that α_t is the coefficient of thermal expansion, δ_{ij} is the Kronecker delta, ρ is the mass density, C_E is the specific heat at the constant strain, k is the thermal conductivity, η^* is entropy per unit mass, k^* is a constant, and q_{ij} are the components of the first heat flux moment vector, we write the equation of continuity for the charges in the body in the form

$$\dot{\rho}_e + \nabla \cdot (\rho_e v_i) = 0, \tag{15}$$

where the velocity of the charges has the components v_i.

Let us now consider that the charge density is a function that does not depend on spatial variables, but only on time variable. Thus, Equation (15) will reduce to

$$\dot{\rho}_e + \rho_e \nabla \cdot (v_i) = 0. \tag{16}$$

We will assume that the charges have the speed of components v_i, which are proportional to the components of the velocity for particles $\dot{u}_i$, so that we can write

$$v_i = p_0 \dot{u}_i, \tag{17}$$

which gives

$$\nabla \cdot v_i = p_0 \nabla \cdot \dot{u}_i = p_0 \dot{e}, \tag{18}$$

where p_0 is a positive constant (non-dimensional).

If we take into account Equation (18), from Equation (16), we are led to

$$\dot{\rho}_e = -\rho_e p_0 \dot{e}, \tag{19}$$

which gives

$$\int \frac{d\rho_e}{\rho} = -p_0 \int de. \tag{20}$$

Hence, we obtain

$$\rho_e = \rho_e^0 \exp(-p_0 e) \simeq \rho_e^0 (1 - p_0 e), \tag{21}$$

where ρ_e^0 is the charge density when the strain vanishes.

Then, we obtain

$$\dot{\rho}_e = -\rho_e^0 (1 - p_0 e) p_0 \dot{e}. \tag{22}$$

While taking into account the Equation (22), from Equation (14) we deduce that the Fourier's law, in its generalized form, receives the form:

$$q_{i,i} = -\left[k T_{,ii} + k^* \dot{T}_{,ii}\right] + M \rho_e^0 (1 - p_0 e) p_0 \dot{e}. \tag{23}$$

In the case of null heat supply, the balance energy becomes

$$\rho T_0 \dot{\eta}^* = - \ q_{i,i}. \tag{24}$$

Taking into account Equations (9) and (23), from Equation (24), we deduce that the equation of heat conduction can be written in the form

$$k T_{,ii} + k^* \dot{T}_{,ii} - m T_0 \dot{\phi} = \rho \ \ C_e \ddot{T} + \beta \ \ T_0 \ddot{u}_{i,i} + M \rho_e^0 (1 - p_0 e) p_0 \dot{e}. \tag{25}$$

This equation can be substitute by an approximate form

$$k T_{,ii} + k^* \dot{T}_{,ii} - m T_0 \dot{\phi} = \rho \ \ C_e \ddot{T} + \beta T_0 \ddot{u}_{i,i} + M \rho_e^0 p_0 \dot{e}. \tag{26}$$

As a consequence, we can obtain the stress components in a simplified form. Accordingly, from Equations (6), (10), and (11), we are led to

$$\sigma_{xx} = \lambda \left[\frac{\partial u}{\partial x} + \frac{\partial v}{\partial y}\right] + 2\mu \frac{\partial u}{\partial x} + \lambda_0 \phi - \beta T - L^*, \tag{27}$$

$$\sigma_{yy} = \lambda \left[\frac{\partial u}{\partial x} + \frac{\partial v}{\partial y}\right] + 2\mu \frac{\partial v}{\partial y} + \lambda_0 \phi - \beta T - L^*, \tag{28}$$

$$\sigma_{zz} = \lambda \left[\frac{\partial u}{\partial x} + \frac{\partial v}{\partial y}\right] + \lambda_0 \phi - \beta T - L^*, \tag{29}$$

$$\sigma_{xy} = (\mu + \frac{L^*}{2}) \frac{\partial u}{\partial y} + (\mu - \frac{L^*}{2}) \frac{\partial v}{\partial x}, \tag{30}$$

$$\sigma_{yx} = (\mu + \frac{L^*}{2})\frac{\partial v}{\partial x} + (\mu - \frac{L^*}{2})\frac{\partial u}{\partial y}, \sigma_{xz} = \sigma_{yz} = 0. \tag{31}$$

The equations of motion, taking into account the Lorentz force

$$\sigma_{ji,j} + F_i = \rho u_{i,tt}. \tag{32}$$

The Lorentz force is given by

$$F_i = \mu_0(\boldsymbol{J} \times \boldsymbol{H})_i. \tag{33}$$

The current density vector $\boldsymbol{J}$ is parallel to electric intensity vector $\boldsymbol{E}$, thus $\boldsymbol{J} = (J_1, J_2, 0)$.
The Ohm's law (5) after linearization gives

$$J_1 = \sigma_0(E_1 + \mu_0 H_0 \dot{v}), \quad J_2 = \sigma_0(E_2 - \mu_0 H_0 \dot{u}). \tag{34}$$

Equations (1), (4), and (34) give

$$\frac{\partial h}{\partial y} = \sigma_0(E_1 + \mu_0 H_0 \frac{\partial v}{\partial t}) + \varepsilon_0 \frac{\partial E_1}{\partial t}, \tag{35}$$

$$\frac{\partial h}{\partial x} = -\sigma_0(E_1 - \mu_0 H_0 \frac{\partial u}{\partial t}) - \varepsilon_0 \frac{\partial E_2}{\partial t}. \tag{36}$$

From Equations (2) and (5), we get

$$\frac{\partial E_1}{\partial y} - \frac{\partial E_2}{\partial x} = \mu_0 \frac{\partial h}{\partial t}. \tag{37}$$

From Equations (33) and (34), we obtain

$$F_1 = \sigma_0 \mu_0 H_0 (E_2 - \mu_0 H_0 \frac{\partial u}{\partial t}), F_2 = -\sigma_0 \mu_0 H_0 (E_1 + \mu_0 H_0 \frac{\partial v}{\partial t}), F_3 = 0. \tag{38}$$

From Equations (27)–(32) and (38), we get

$$(\mu - \frac{L^*}{2})\nabla^2 u + (\lambda + \mu + \frac{L^*}{2})\frac{\partial e}{\partial x} + b\frac{\partial \phi}{\partial x} - \beta \frac{\partial T}{\partial x} + \sigma_0 \mu_0 H_0 (E_2 - \mu_0 H_0 \frac{\partial u}{\partial t}) = \rho \frac{\partial^2 u}{\partial t^2} \tag{39}$$

$$(\mu - \frac{L^*}{2})\nabla^2 v + (\lambda + \mu + \frac{L^*}{2})\frac{\partial e}{\partial y} + b\frac{\partial \phi}{\partial y} - \beta \frac{\partial T}{\partial y} - \sigma_0 \mu_0 H_0 (E_1 + \mu_0 H_0 \frac{\partial v}{\partial t}) = \rho \frac{\partial^2 v}{\partial t^2}, \tag{40}$$

in which we used the notation $e = \frac{\partial u}{\partial x} + \frac{\partial v}{\partial y}$.
For the equation of the equilibrated forces, we obtain

$$\rho \psi \phi_{,tt} = h_{i,i} + g. \tag{41}$$

Also, while taking into account Equations (7), (8), and (41), we are led to

$$\alpha\, \phi_{,jj} - \lambda_0 u_{i,i} - \xi_1 \phi - \omega_0\, \phi_{,t} + m\, T = \rho \psi \ddot{\phi}. \tag{42}$$

Let us define the non-dimensional sizes

$$(x'_i, u'_i) = \frac{w_1^*}{c_1}(x_i, u_i), (t', t'_0) = w_1^*(t, t_0), \phi' = \frac{\psi\, w_1^{*2}}{c_1^2}\phi, \sigma'_{ij} = \frac{\sigma_{ij}}{\mu}, p'_1 = \frac{p_1}{\mu}, L^{*'} = \frac{L^*}{\mu},$$

$$\theta' = \frac{T - T_0}{T_0}, h' = \frac{w_1^*}{\sigma_0 H_0 \mu_0 c_1^2} h, E'_i = \frac{w_1^*}{\sigma_0 H_0^2 \mu_0 c_1^2} E_i, \tag{43}$$

where $w_1^* = \frac{\rho c_e c_1^2}{K}$, $c_1^2 = \frac{\lambda+2\mu}{\rho}$.

For dimensionless sizes that are defined in Equation (43), we can write the above basic equations in the following from

$$a_1\nabla^2 u + a_2\frac{\partial e}{\partial x} + a_3\frac{\partial \phi}{\partial x} - a_4\frac{\partial \theta}{\partial x} + a_5(a_6 E_2 - \frac{\partial u}{\partial t}) = a_7\frac{\partial^2 u}{\partial t^2}, \tag{44}$$

$$a_1\nabla^2 v + a_2\frac{\partial e}{\partial y} + a_3\frac{\partial \phi}{\partial y} - a_4\frac{\partial \theta}{\partial y} - a_5(a_6 E_1 + \frac{\partial v}{\partial t}) = a_7\frac{\partial^2 v}{\partial t^2}, \tag{45}$$

$$(\nabla^2 - a_8 - a_9\frac{\partial}{\partial t} - a_{10}\frac{\partial^2}{\partial t^2})\phi - a_{11}e + a_{12}\theta = 0, \tag{46}$$

$$[(k + k^* w_1^*\frac{\partial}{\partial t})\nabla^2 - a_{13}\frac{\partial^2}{\partial t^2}]\theta + a_{14}\frac{\partial \phi}{\partial t} - \beta c_1^*\frac{\partial^2 e}{\partial t^2} - M_0\frac{\partial e}{\partial t} = 0, \tag{47}$$

$$\frac{\partial h}{\partial y} = a_{15}E_1 + a_{16}\frac{\partial E_1}{\partial t} + \frac{\partial v}{\partial t}, \tag{48}$$

$$\frac{\partial h}{\partial x} = -a_{15}E_2 - a_{16}\frac{\partial E_2}{\partial t} + \frac{\partial u}{\partial t}, \tag{49}$$

$$\frac{\partial E_1}{\partial y} - \frac{\partial E_2}{\partial x} = \frac{\partial h}{\partial t}, \tag{50}$$

by dropping the dashed, for convenience. Here, $M_0 = \frac{M\rho_e^0 p_0 c_1^2}{w_1^* T_0}$, is the Peltier coefficient at T_0 and $a_1 = \mu - \frac{L^*\mu}{2}$, $a_2 = \lambda + \mu + \frac{L^*\mu}{2}$, $a_3 = \frac{bc_1^2}{\psi w_1^{*2}}$, $a_4 = \beta T_0$, $a_5 = \frac{\mu_0^2 H_0^2 \sigma_0 c_1^2}{w_1^*}$, $a_6 = \frac{\mu_0\sigma_0 c_1^2}{w_1^*}$, $a_7 = \rho c_1^2$, $a_8 = \frac{\xi_1 c_1^2}{\alpha w_1^{*2}}$, $a_9 = \frac{w_0 c_1^2}{\alpha w_1^*}$, $a_{12} = \frac{m\psi T_0}{\alpha}$, $a_{13} = \rho C_e c_1^2$, $a_{14} = \frac{mc_1^4}{\psi w_1^{*3}}$, $a_{15} = \frac{\sigma_0\mu_0 c_1^2}{w_1^*}$, $a_{16} = \mu_0\varepsilon_0 c_1^2$, $a_{10} = \frac{\rho\psi c_1^2}{\alpha}$, $a_{11} = \frac{\lambda_0\psi}{\alpha}$.

From Equations (44) and (45), we obtain

$$[(a_1 + a_2)\nabla^2 - a_7\frac{\partial}{\partial t} - a_5\frac{\partial^2}{\partial t^2}]\, e + a_3\nabla^2\phi - a_4\nabla^2\theta - a_6 a_5\frac{\partial h}{\partial t} = 0. \tag{51}$$

From Equations (48) and (49), we obtain

$$(\nabla^2 - a_{15}\frac{\partial}{\partial t} - a_{16}\frac{\partial^2}{\partial t^2})h - \frac{\partial e}{\partial t} = 0. \tag{52}$$

3. The Solution of the Problem

3.1. Decomposition by Normal Mode Analysis

Using the normal mode analysis, we can decompose the solution of the above physical parameters in the following form

$$[e, \theta, \phi, h, \sigma_{ij}](x, y, t) = [e^*, \theta^*, \phi^*, h^*, \sigma_{ij}^*](y)\exp[i(a\,x - \omega\,t)], \tag{53}$$

in which $e^*, \phi^*, \theta^*, h^*, \sigma_{ij}^*$ are the amplitudes of the respective fields, $i = \sqrt{-1}$, ω is the frequency, and a is the wave number.

By taking into account Equation (53) in Equations (46), (47), (51), and (52), we are led to

$$(r_1 D^2 - r_2)\, e^* + a_3(D^2 - a^2)\phi^* - a_4(D^2 - a^2)\theta^* + r_3 h^* = 0, \tag{54}$$

$$(D^2 - r_4)\,\phi^* - a_{11}e^* + a_{12}\theta^* = 0, \tag{55}$$

$$(r_5 D^2 - r_6)\,\theta^* + r_7\phi^* + r_8 e^* = 0, \tag{56}$$

$$(D^2 - r_9)\, h^* + i\omega e^* = 0, \tag{57}$$

where $r_1 = a_1 + a_2, r_2 = ra^2 - i\omega\, a_5 - a_7\omega^2, r_3 = i\omega\, a_6 a_5, r_4 = a^2 + a_8 - i\omega a_9 - a_{10}\omega^2, r_5 = k - i\omega k^* w^*$, $r_6 = r_5 a^2 - a_{13}\omega^2, r_7 = i\omega\, a_{14}, r_8 = \beta\omega^2 c_1^2 - i\omega M_0$, and $r_9 = a^2 - i\omega\, a_{15} - a_{10}\omega^2$.

Eliminating (55), we get the following ordinary Equation (52) between $e^*(y)$ $\phi^*(y)$, $\theta^*(y)$, the differential Equation satisfied by $h^*(y)$:

$$\left(D^8 - N_1\, D^6 + N_2\, D^4 - N_3\, D^2 + N_4\right)\{h^*(y), \phi^*(y), e^*(y), \theta^*(y)\} = 0. \tag{58}$$

We can write the Equation (58) in a decomposed form, as follows

$$(D^2 - k_1^2)(D^2 - k_2^2)(D^2 - k_3^2)(D^2 - k_4^2)\{h^*(y), \phi^*(y), e^*(y), \theta^*(y)\} = 0, \tag{59}$$

where, $k_n^2\,(n = 1, 2, 3, 4)$ are roots of the characteristic equation of Equation (58) and $s_1 = r_5 r_9 + r_4 r_5 + r_6$, $s_2 = r_6 r_9 + r_4 r_5 r_9 - a_{12} r_7 + r_6 r_4$, $s_3 = r_4 r_6 r_9 + a_{12} r_7 r_9$, $s_4 = r_5 r_6 - a_{12} r_8 + r_6$, $s_5 = a_{11} r_6 r_9 - a_{12} r_8 r_9$, $s_6 = r_8 r_9 + r_4 r_8 - a_{11} r_3$, $s_7 = r_8 r_4 r_9 - a_{11} r_7 r_9$, $s_8 = r_6 + r_4 r_5$, $s_9 = r_4 r_6 - a_{12} r_7$, $s_{10} = \frac{1}{r_1 r_5}$, $N_1 = s_{10}(r_1 s_1 + r_2 r_5 - a_3 a_{11} r_5 + a_4 r_8)$, $N_2 = s_{10}(r_1 s_2 + r_2 s_1 - a_3 a_{11} r_5 a^2 - a_3 s_4 + a_4 s_6 + a_4 r_8 a^2 - i\omega r_3 r_5)$, $N_3 = s_{10}(r_1 s_3 + r_2 s_2 - a_3 s_5 - a_3 s_4 a^2 + a_4 s_7 + a_4 s_6 a^2 - i\omega r_3 r_8)$, and $N_4 = s_{10}(r_2 s_3 - a_3 s_5 a^2 + a_4 s_7 a^2 - i\omega r_3 r_9)$.

The general solutions of the Equation (59), bound at $y \to \infty$,

$$e(x, y, t) = \sum_{n=1}^{4} R_n \exp[-k_n y + i(ax - \omega t)], \tag{60}$$

$$h(x, y, t) = \sum_{n=1}^{4} H_{1n} R_n \exp[-k_n y + i(ax - \omega t)], \tag{61}$$

$$\theta(x, y, t) = \sum_{n=1}^{4} H_{2n} R_n \exp[-k_n y + i(ax - \omega t)], \tag{62}$$

$$\phi(x, y, t) = \sum_{n=1}^{4} H_{3n} R_n \exp[-k_n y + i(ax - \omega t)], \tag{63}$$

where

$$H_{1n} = \frac{-i\omega}{k_n^2 - s_9}, H_{2n} = \frac{-r_8(k_n^2 - r_4) - r_7 a_{11}}{(k_n^2 - r_4)(r_5 k_n^2 - r_6) - r_7 a_{12}}, H_{3n} = \frac{a_{11} - a_{12} H_{2n}}{k_n^2 - r_4}. \tag{64}$$

3.2. Boundary Conditions

In the following, we will consider some boundary conditions on the surface of Equation $y = 0$, which will help us to determine the above constants R_1, R_2, R_3 and R_4.

3.2.1. The mechanical boundary condition

The mechanical boundary condition that the bounding plane to the surface $y = 0$ has zero strain, so we have

$$e(x, 0, t) = 0$$

3.2.2. The Boundary Restriction of Heat

We assume that the boundary surface of the body is subject to a thermal shock described by the function

$$\theta(x, 0, t) = \theta_0 \exp(i(ax - \omega t)), \tag{65}$$

where θ_0 is constant.

3.2.3. Voids Conditions

$$\frac{\partial \phi}{\partial y} = 0. \tag{66}$$

3.2.4. The Boundary Restriction for Electromagnetic Field

On the surface of the half-space $h(x,0,t) = h^*$, we consider that the electromagnetic field intensity is a continuous function. Here, the intensity of the magnetic field in free space is h^*.

We now assume there is no magnetic or electric field in the free space, that is,

$$h(x,0,t) = h^* = 0. \tag{67}$$

In order to obtain the constants R_1, R_2, R_3 and R_4, we will use the dimensionless size ${\theta'}_0 = \frac{\theta_0}{T_0}$ and the expressions of the variables into the boundary restrictions imposed above. Additionally, we will use the normal mode analysis in order to obtain the system of equations

$$\sum_{n=1}^{4} R_n = 0, \tag{68}$$

$$\sum_{n=1}^{4} H_{2n} R_n = \theta_0, \tag{69}$$

$$\sum_{n=1}^{4} k_n H_{3n} R_n = 0, \tag{70}$$

$$\sum_{n=1}^{4} H_{1n} R_n = 0. \tag{71}$$

after suppressing the primes.

After applying the inverse of matrix method for the above equations, we get the values of the constants $R_n (n = 1,2,3,4)$, hence; we obtain the expressions of strain, magnetic intensity, temperature distribution and the change in the volume fraction field for the generalized thermoelastic medium with voids.

4. Special Cases

4.1. Pores Neglect

First, we will neglect the presence of the voids, that is, we have $(\alpha = \lambda_0 = \xi_1 = \omega_0 = m = \psi = 0)$.

While putting $(\alpha = \lambda_0 = \xi_1 = \omega_0 = m = \psi = 0)$ in Equations (54)–(57), we get:

$$(r_1 D^2 - r_2)\, e^* - a_4 (D^2 - a^2)\theta^* + r_3 h^* = 0, \tag{72}$$

$$(r_5 D^2 - r_6)\, \theta^* + r_8 e^* = 0, \tag{73}$$

$$(D^2 - r_9)\, h^* + i\omega\, e^* = 0. \tag{74}$$

Eliminating e^*, θ^*, and h^* among Equations (72)–(74), we obtain the following sixth order differential Equation, which is satisfied by $e^*(y)$, $\theta^*(y)$ and $h^*(y)$

$$[D^6 - B_1\, D^4 + B_2\, D^2 - B_3]\{e^*(y), \theta^*(y), h^*(y)\} = 0, \tag{75}$$

where $s_{10} = \frac{1}{r_1 r_5}$, $B_2 = s_{10}[r_1 r_6 r_9 + r_2 r_5 r_9 + r_2 r_6 - r_8 a_4 (r_9 + a^2) + i\omega r_3 r_5]$, $B_1 = s_{10}(r_1 r_9 r_5 + r_1 r_6 + r_2 r_5 - r_8 a_4)$, $B_3 = s_{10}(r_2 r_5 r_9 - r_8 a_4 r_9 a^2 + i\omega r_3 r_6)$.

The solutions of Equation (75) are

$$(e^*, h^*, \theta^*)(y) = \sum_{n=1}^{3} (1, H_{4n}, H_{5n}) R_n^* \exp(-\alpha_n^* y), \tag{76}$$

where α_n^{*2} $(n = 1, 2, 3)$ are the roots of the characteristic equation of Equation (75) and $H_{4n} = \frac{-i\omega}{\alpha_n^{*2} - r_9}$, $H_{5n} = \frac{-r_8}{r_5 \alpha_n^{*2} - r_6}$.

The expressions for the strain, the induced magnetic field, and the temperature field in the generalized initially stressed the electro-magneto-thermoelastic half-space solid with voids are:

$$(e^*, h^*, \theta^*)(y) = \sum_{n=1}^{3} (1, H_{4n}, H_{5n}) R_n^* \exp(-\alpha_n^* y + i\,(a\,x - \omega t)). \tag{77}$$

We wish to determine the above coefficients R_n^*, $(n = 1, 2, 3)$.

To this end, we will keep in mind the boundary conditions in Equations (64), (65), and (67), and we will use the method of inverse of the matrix, as following:

$$\begin{pmatrix} R_1^* \\ R_2^* \\ R_3^* \end{pmatrix} = \begin{pmatrix} 1 & 11 & \\ H_{51} & H_{52} & H_{53} \\ H_{41} & H_{42} & H_{43} \end{pmatrix}^{-1} \begin{pmatrix} 0 \\ \theta_0 \\ 0 \end{pmatrix}. \tag{78}$$

4.2. Neglecting the Initial Stress

By taking $(L^* = 0)$ in the governing equations, the corresponding expressions of the physical variables can be obtained without initial stress.

5. Numerical Results and Discussion

For numerical computations, following Dhaliwal and Singh [28], magnesium material was chosen for the purposes of numerical evaluations. All of the units of parameters that were used in the calculation are given in SI units. The constants were taken as $\lambda = 2.17 \times 10^{10}$ N/m^2, $\mu = 3.278 \times 10^{10}$ N/m^2,$k = 1.7 \times 10^2$ W/m·deg, $\rho = 1.74 \times 10^3$ Kg/m^3, $\beta = 2.68 \times 10^6$ N/m^2·deg, $C_e = 1.04 \times 10^3$ J/Kg·deg, $\omega_1^* = 3.58 \times 10^{11}$ /s, $\alpha_t = 1.78 \times 10^{-5}$ N/m^2 and T_0 = 298 K.

The voids parameters are $\psi = 1.753 \times 10^{-15}$ m^2, $\alpha = 3.688 \times 10^{-5}$ N, $\xi_1 = 1.475 \times 10^{10}$ N/m^2, $\lambda_0 = 1.13849 \times 10^{10}$ N/m^2, $m = 2 \times 10^6$ N/m^2·deg and $\omega_0 = 0.0787 \times 10^{-3}$ N/m^{2}s.

The Magnetic field parameters are $\varepsilon_0 = 10^{-9}/(36\pi)\, F/M$, $\mu_0 = 4\pi \times 10^{-7} H/M$, $H_0 = 10^5 A/M$ and $\sigma_0 = 9.36 \times 10^5$ Col^2/Cal·cm·sec.

The comparisons were carried out for $a = 0.7$ m, $\theta_0 = 0.1$ k, $\omega = \chi_0 + i\chi_1$, $\chi_0 = 2$ rad/s, $\chi_1 = 0.09$ rad/s, $x = 0.2$ m, and $0 \le y \le 4$ m.

Since, we have $\exp(\omega t) = [\cos(\chi_1 t) + i \sin(\chi_1 t)] \exp(\chi_0 t)$, and for small values of time we can take $\omega = \chi_0$, which is a real constant.

The above comparisons have been made in the context of two (G-N) theories of type II and III, in three situations:

(i) whether we have an initial stress or not [L^* =0 and 10^5 at M_0=0.5 and H_0=10^5];
(ii) whether we have a Thomson effect or not [M_0 =0 and 0.5 at H_0=10^5 and L^*=10^5];
(iii) whether we have some void parameters or not $[M_0 = 0.5,\ H_0 = 10^5\ and\ L^* = 10^5]$.

Case i: In the Figures 1–4, we made the calculations for $t = 0.2$, at $x = 0.2$. The values of the deformation e, the values of the temperature θ, the electromagnetic field h, and the values of the voids

function ϕ are graphically represented, for different values of y in some graphs of two-dimensional space. In these figures, we use the solid lines for the results in the case without initial stress for the (G-N) theory of type II. For the results in the case of the (G-N) theory of type II with initial stress, we have used the large dashes line. In the case without initial stress for the (G-N) theory of type III, we have used the small dashes. Finally, for the results in the case with initial stress for the (G-N) theory of type III, we have used the small dashes line with dot.

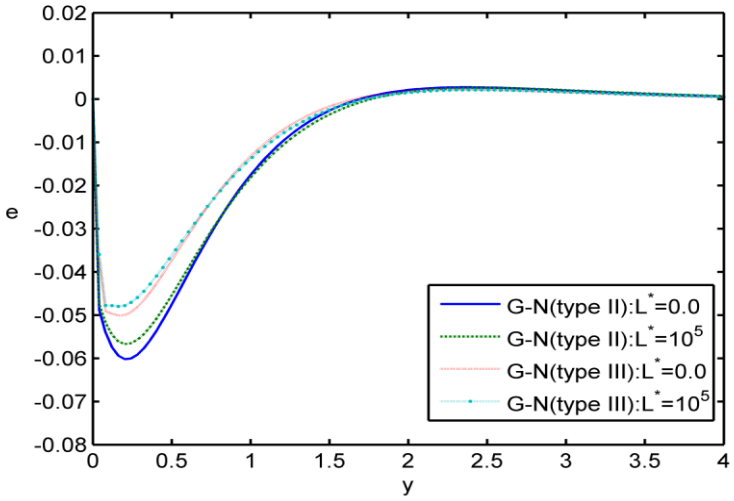

Figure 1. The strain e distribution at $M_0 = 0.5$ and $H_0 = 10^5$.

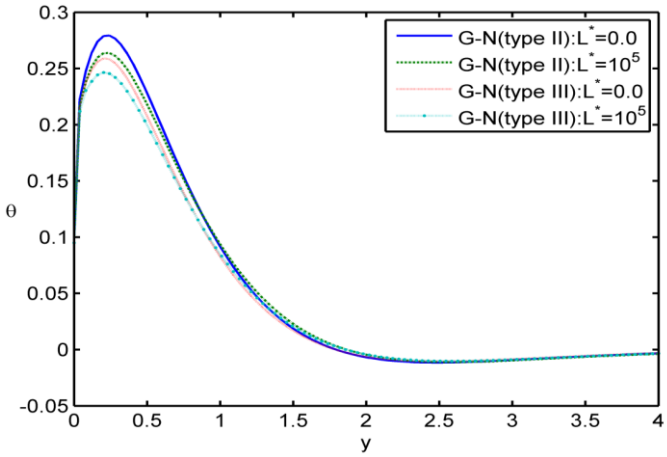

Figure 2. The temperature θ distribution at $M_0 = 0.5$ and $H_0 = 10^5$.

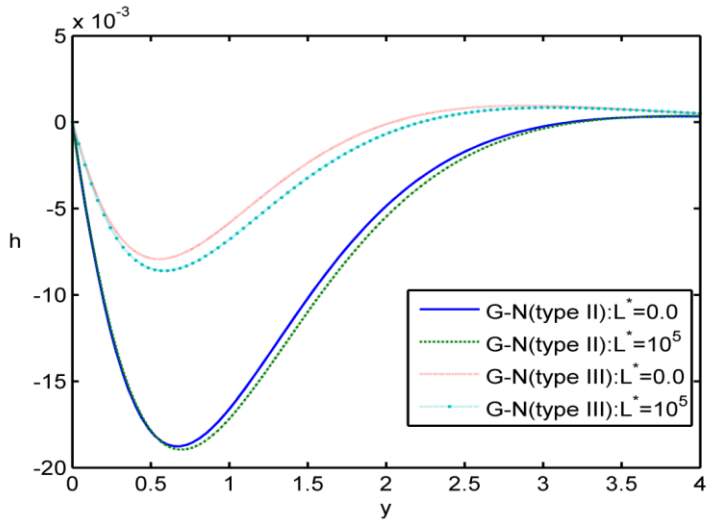

Figure 3. The induced magnetic field h distribution at $M_0 = 0.5$, and $H_0 = 10^5$.

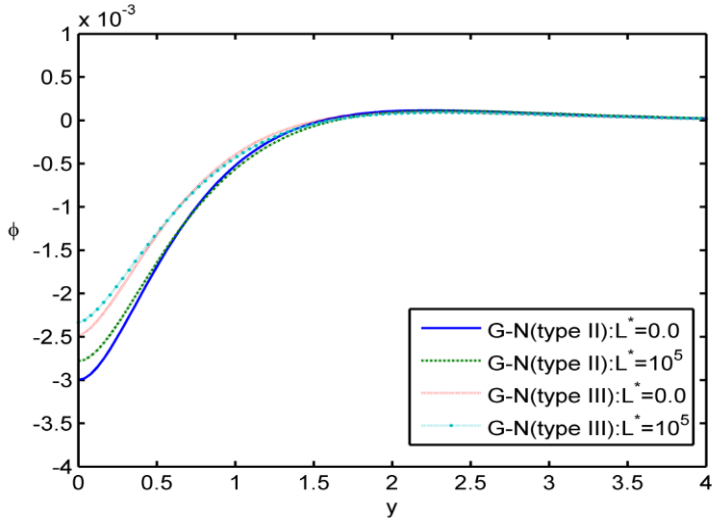

Figure 4. The change in the volume fraction field ϕ distribution at $M_0 = 0.5$ and $H_0 = 10^5$.

Figure 1 depicts the variation of the strain e versus y. The magnitude of the strain is found to be large for the G-N theory of type III. It can be seen that the initial stress shows an increasing effect on the magnitude of strain. In Figure 2, the parameter for the initial stress is decreasing as an effect. Additionally, when the initial stress parameter L^* is increasing, the value of the temperature θ is decreasing. Figure 3 shows the variation of the induced magnetic field h versus y. The value of strain is found to be large for the theory of G-N of type III. It can be seen that the presence of the initial stress shows a decreasing effect on the magnitude of the induced magnetic field. Figure 4 expresses the distribution of the change in the volume fraction field ϕ versus y. It was observed that the initial stress has a great effect on the distribution of ϕ.

Case ii: In the Figures 5–8, calculations were made for $M_0 = 0.0, 0.5$ at $H_0 = 10^5$, and $t = 0.2$. The strain e, the temperature θ, the electromagnetic field h and the voids function ϕ are graphically represented in some of the graphs for different values of y. Here, the solid lines is for results in the G-N theory of type II at $M_0 = 0.0$, which gives the classical Fourier's law of heat conduction, the large dashes line is for results in the type II G-N theory at $M_0 = 0.5$, which gives the generalized Fourier's law of heat conduction. We also use a small dashes line for the results for the type III G-N theory in the case $M_0 = 0.0$, while the line with small dashes and the dot is for results for the type III G-N theory for $M_0 = 0.5$. Figure 5 is for the effect of M_0 in the case that it exists and we can see that the value of the

deformation e is increasing when M_0 increases with the corresponding difference. Figure 6 is for the value of the temperature θ, which is decreasing for the parameter M_0, which is increasing. In Figure 7, the effect of parameter M_0 exists and the value of the induced magnetic field h increases when the parameter M_0 increases. In Figure 8, the value of the voids function ϕ is increasing for the case that the parameter M_0 is increasing.

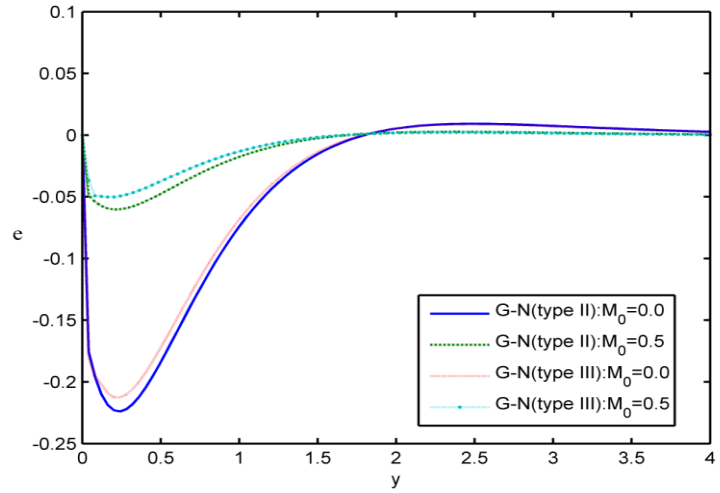

Figure 5. The strain e distribution at $H_0 = 10^5$ and $L^* = 10^5$.

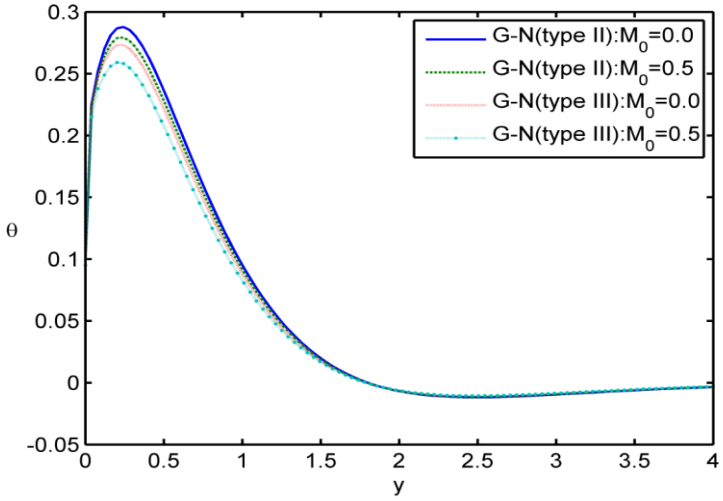

Figure 6. The temperature θ distribution at $H_0 = 10^5$ and $L^* = 10^5$.

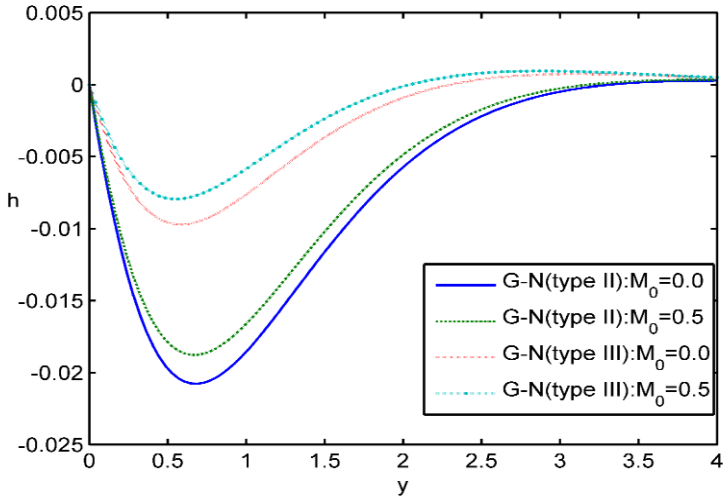

Figure 7. The induced magnetic field h distribution at $H_0 = 10^5$ and $L^* = 10^5$.

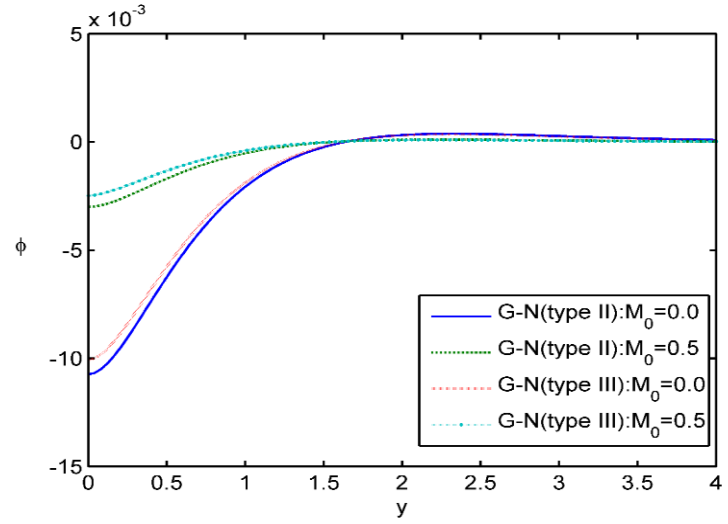

Figure 8. The change in the volume fraction field ϕ distribution at $H_0 = 10^5$ and $L^* = 10^5$.

Case iii: Figures 9–11 present the evolution of the physical sizes with regards to the distance y in 2D during $M_0 = 0.5$, $H_0 = 10^5$, $L^* = 10^5$, and with and without void parameter, in the context of G-N theory of type II and type III G-N theories. In this case of comparison, the solid lines is for results of pore effect 1.9 in the type II G-N theory, the small dashes line is also the voids effect, but in the case of the type III G-N theory. We use a large dashes line for results in the G-N theory of type II by neglecting the effect of pores, while the small dashes line with dot is used for results in the type III G-N theory, neglecting the effect of pores. In Figure 9, we find the repartition of the strain e, and we have a comparison between the values of the strain in the case of the presence of the pores to those in the case of neglecting the voids, in the range $0 \leq y \leq 1.7$; while, the values are the same for two cases at $y \geq 1.7$. Figure 10 illustrates the repartition of the temperature θ, and a comparison between the temperature in the case of presence of pores to those in the case of neglecting the voids, for y in the range $0 < y < 1.9$. In the case $y > 1.9$, the values are the same for two cases. Figure 11 depicts the repartition of the magnetic field h, an the values of the magnetic field h in the case of the presence of pores are compared to those in the case of neglecting the voids, for y in the range $0 \leq y \leq 3$; in the case $y \geq 3$. The values are the same for the two cases.

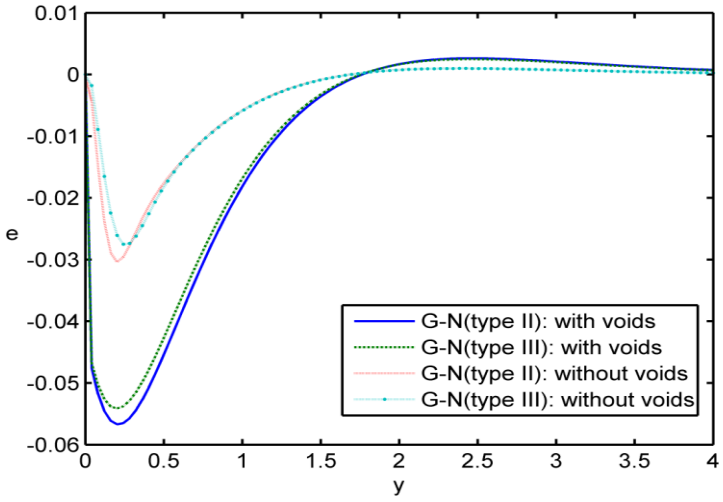

Figure 9. The strain e distribution at $H_0 = 10^5$, $M_0 = 0.5$ and $L^* = 10^5$.

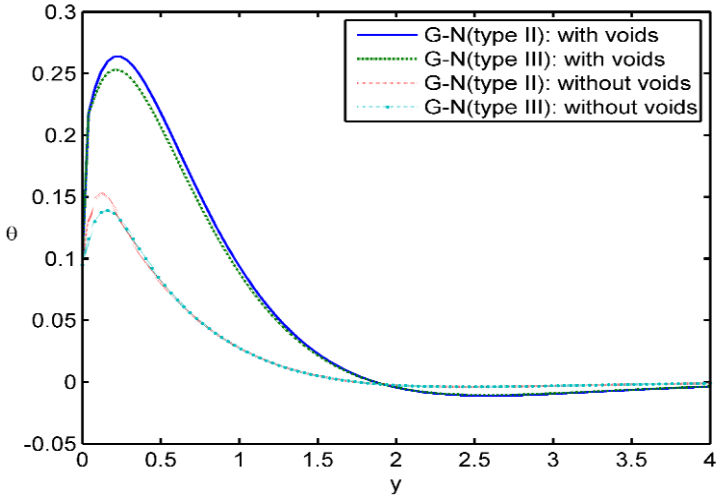

Figure 10. The temperature θ distribution at $H_0 = 10^5$, $M_0 = 0.5$, and $L^* = 10^5$.

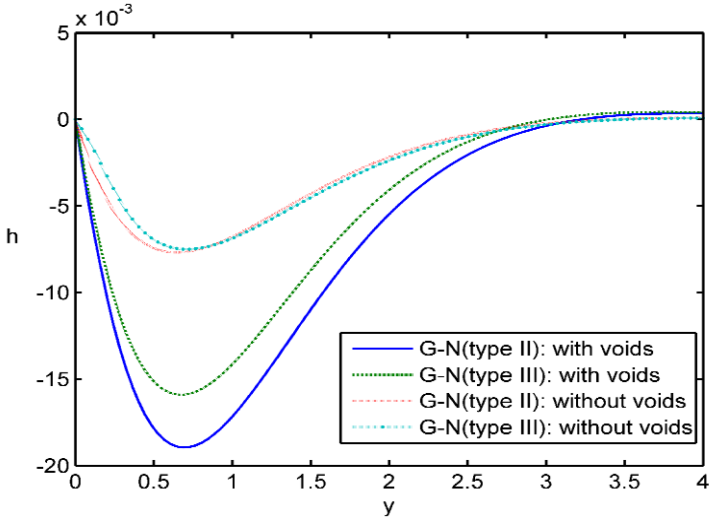

Figure 11. The induced magnetic field h distribution at $H_0 = 10^5$, $M_0 = 0.5$, and $L^* = 10^5$.

Figures 12–15 are giving 3D surface curves for the physical quantities i.e., the strain e, the temperature θ, the magnetic field h, and the voids fuction ϕ for the thermoelastic theory of

electromagnetic bodies with pores, by taking into account the Thomson effect and the effect of the initial stress. The importance of these figures is that they give the dependence of the above physical sizes regarding the vertical component of distance.

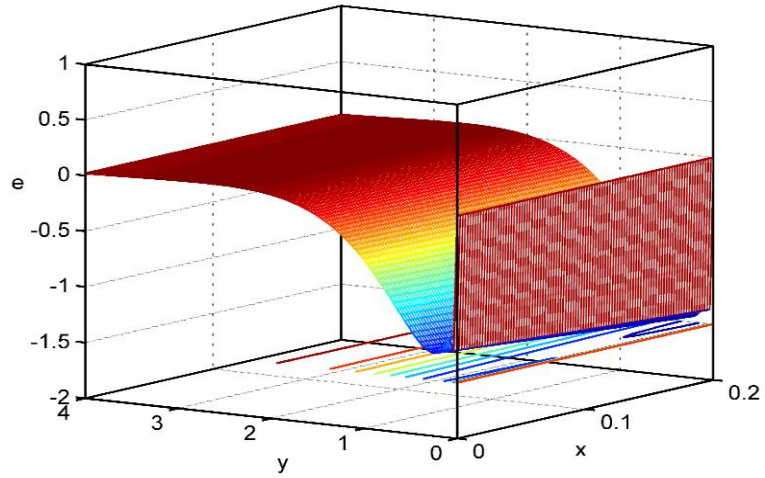

Figure 12. Three-dimensional (3D) curve distribution of the strain e versus the distances at: $M_0 = 0.5$, $H_0 = 10^5$, and $L^* = 10^5$.

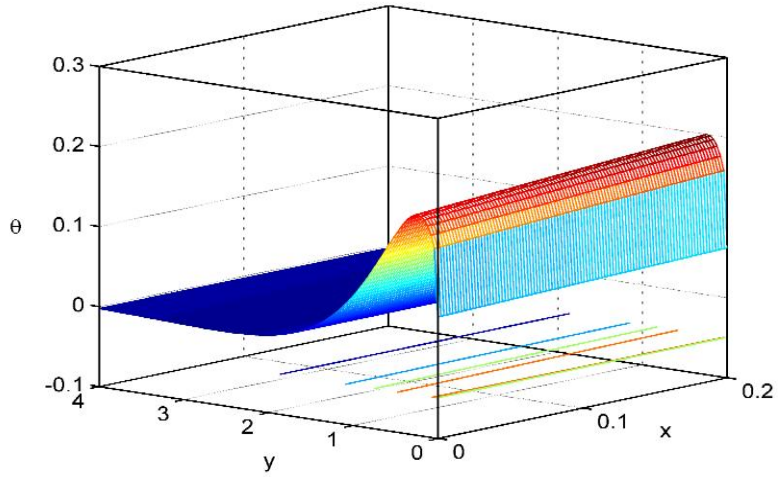

Figure 13. 3D Curve distribution of the temperature θ versus the distances, at: $M_0 = 0.5$, $H_0 = 10^5$ and $L^* = 10^5$.

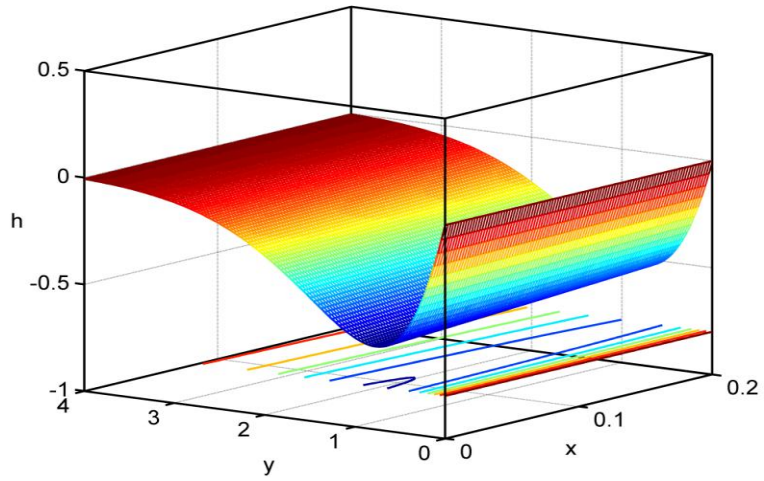

Figure 14. 3D Curve distribution of the induced magnetic field h versus the distances, at: $M_0 = 0.5$, $H_0 = 10^5$ and $L^* = 10^5$.

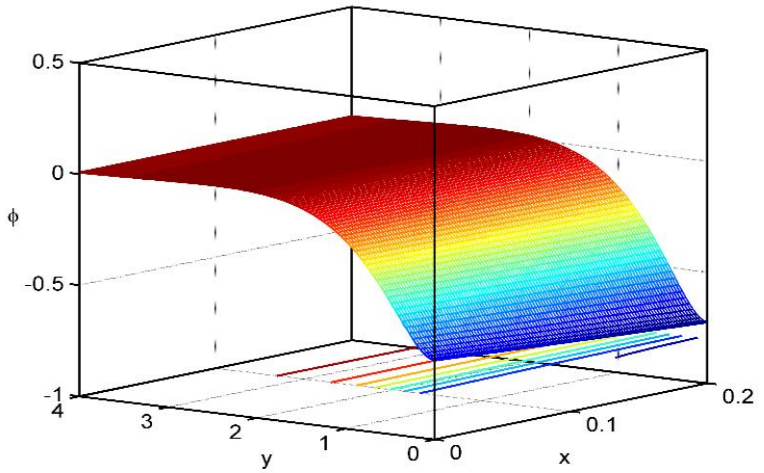

Figure 15. 3D Curve distribution of the change in the volume fraction field ϕ versus the distances, at: $M_0 = 0.5$, $H_0 = 10^5$ and $L^* = 10^5$.

6. Conclusions

The results concluded from the above analysis can be summarized, as follows:

(1) We have derived the field equations of homogeneous, isotropic, electro-magneto-thermo- porous elastic half-plane with the Thomson effect and initial stress.
(2) The analytical solutions that are based upon normal mode analysis for the thermoelastic problem in solids have been developed and utilized.
(3) The presence of initial stress, void parameters, and Thomson effect play significant roles in all of the physical quantities.
(4) The value of all physical quantities converges to zero with the increase in distance y and all of the functions are continuous.
(5) The deformation of a body depends on the nature of the applied forces and Thomson effect, as well as the type of boundary conditions.

Author Contributions: All three authors conceived the framework and structured the whole paper, checked the results of the paper and completed the revision of the article. The authors have equally contributed to the elaboration of this manuscript. All authors have read and approved the final manuscript.

Funding: This research received no external funding.

Acknowledgments: The authors would like to thank the anonymous referee for the comments that helped us improve this article.

Conflicts of Interest: The authors declare no conflict of interest.

References

1. Green, A.E.; Naghdi, P.M. A re-examination of the basic postulates of thermo-mechanics. *Proc. R. Soc. Lond. A* **1991**, *432*, 171–194. [CrossRef]
2. Green, A.E.; Naghdi, P.M. On undamped heat wave in elastic solids. *J. Therm. Stresses* **1992**, *15*, 253–264. [CrossRef]
3. Green, A.E.; Naghdi, P.M. Thermoelasticity without energy dissipation. *J. Elast.* **1993**, *31*, 189–209. [CrossRef]
4. Sharma, J.N.; Chouhan, R.N. On the problems of body forces and heat sources in thermoelasticity without energy dissipation, Indian. *J. Pure Appl. Math.* **1999**, *30*, 595–610.
5. Liang, M.; Liu, Y.; Xiao, B.; Yang, S.; Wang, Z.; Han, H. An analytical model for the transverse permeability of gas diffusion layer with electrical double layer effects in proton exchange membrane fuel cells. *Int. J. Hydrogen Energy* **2018**, *43*, 17880–17888. [CrossRef]
6. Xiao, B.; Zhang, X.; Wang, W.; Long, G.; Chen, H.; Kang, H.; Ren, W. Afractal model for water flow through unsaturated porous rocks. *Fractals* **2018**, *26*, 1840015. [CrossRef]
7. Hassan, M.; Marin, M.; Alsharif, A.; Ellahi, R. Convective heat transfer flow of nanofluid in a porous medium over wavy surface. *Phys. Lett. A Gen. At. Solid State Phys.* **2018**, *382*, 2749–2753. [CrossRef]
8. Long, G.; Liu, S.; Xu, G.; Won, S.W. A perforation-erosion model for hydraulic-fracturing applications. *SPE Prod. Oper.* **2018**, *33*, 770–783. [CrossRef]
9. Xiao, B.; Chen, H.; Xiao, S.; Cai, J. Research on relative permeability of nanofibers with capillary pressure effect by means of fractal-monte Carlo technique. *J. Nanosci. Nanotechnol.* **2017**, *17*, 6811–6817. [CrossRef]
10. Xiao, B.; Wang, W.; Fan, J.; Chen, H.; Hu, X.; Zhao, D.; Zhang, X.; Ren, W. Optimization of the fractal-like architecture of porous fibrous materials related to permeability, diffusivity and thermal conductivity. *Fractals* **2017**, *25*, 1750030. [CrossRef]
11. Nunziato, J.W.; Cowin, S.C. A non-linear theory of elastic materials with voids. *Arch. Rat. Mech. Anal.* **1979**, *72*, 175–201. [CrossRef]
12. Cowin, S.C.; Nunziato, J.W. Linear theory of elastic materials with voids. *J. Elast.* **1983**, *13*, 125–147. [CrossRef]
13. Puri, P.; Cowin, S.C. Plane waves in linear elastic materials with voids. *J. Elast.* **1985**, *15*, 167–183. [CrossRef]
14. Iesan, D. A theory of thermoelastic materials with voids. *Acta Mech.* **1986**, *60*, 67–89. [CrossRef]
15. Cicco, S.D.; Diaco, M. A theory of thermoelastic material with voids without energy dissipation. *J. Therm. Stress.* **2002**, *25*, 493–503. [CrossRef]
16. Othman, M.I.A.; Edeeb, E.R.M. The effect of rotation on thermoelastic medium with voids and temperature dependent under three theories. *J. Eng. Mech.* **2018**, *144*, 04018003. [CrossRef]
17. Montanaro, A. On singular surfaces in isotropic linear thermoelasticity with initial stress. *J. Acoust. Soc. Am.* **1999**, *106*, 1586–1588. [CrossRef]
18. Othman, M.I.A.; Abd-Elaziz, E.M. The effect of thermal loading due to laser pulse on generalized thermoelastic medium with voids in dual phase lag model. *J. Therm. Stress.* **2015**, *38*, 1068–1082. [CrossRef]
19. Marin, M. Cesaro means in thermoelasticity of dipolar bodies. *Acta Mechanica* **1997**, *122*, 155–168. [CrossRef]
20. Marin, M.; Oechsner, A. The effect of a dipolar structure on the Holder stability in Green-Naghdi thermoelasticity. *Contin Mech Thermodyn* **2017**, *29*, 1365–1374. [CrossRef]
21. Nowinski, J. *Theory of Thermoelasticity with Applications*; Sijthoff and Noordhoff International Publishers: Alphen Aan Den Rijn, The Netherlands, 1978.
22. Chadwick, P. *Progress in Solid Mechanics*; Hill, R., Sneddon, I.N., Eds.; North Holland Publishing Company: North Holland, Amsterdam, 1960.
23. Hussain, F.; Ellahi, R.; Zeeshan, A. Mathematical models of electromagnetohydrodynamic multiphase flows synthesis with nanosized hafnium particles. *Appl. Sci.* **2018**, *8*, 275. [CrossRef]
24. Bhatti, M.M.; Zeeshan, A.; Ellahi, R.; Ijaz, N. Heat and mass transfer of two-phase flow with Electric double layer effects induced due to peristaltic propulsion in the presence of transverse magnetic field. *J. Mol. Liq.* **2017**, *230*, 237–246. [CrossRef]

25. Othman, M.I.A.; Abd-Elaziz, E.M. Plane waves in a magneto-thermoelastic solids with voids and microtemperatures due to hall current and rotation. *Results Phys.* **2017**, *7*, 4253–4263. [CrossRef]
26. Marin, M.; Craciun, E.M.; Pop, N. Consideration on mixed initial-boundary value problems for micro-polarporous bodies. *Dyn. Syst. Appl.* **2016**, *25*, 175–196.
27. Marin, M.; Craciun, E.M. Uniqueness results for a boundary value problem in dipolar thermoelasticity to model composite materials. *Compos. Part B Eng.* **2017**, *126*, 27–37. [CrossRef]
28. Dhaliwal, R.S.; Singh, A. *Dynamic Coupled Thermoelasticity*; Hindustan Publ. Corp.: New Delhi, India, 1980.